CHAPTER 4. IN VITRO CHARACTERIZATION

Contents

List OF Figure

List of Table

Error! Bookmark not defined.

4.1. Cell-line Studies

Various *in vitro* cell line studies were carried out for further screening of prepared liposomal carriers to achieve maximum gemcitabine uptake inside the cells with desired transfection.

The A549 cell line was procured from National Culture Collection Society (NCCS), Pune. The cells were maintained as monolayer culture in T-25 cell culture flasks, and medium was replaced two times in a week. Cell were sub-cultured at 37°C in a humidified atmosphere (95% air and 5% CO_2) using DMEM medium supplemented with penicillin (100 units/ml), streptomycin (100 µg/ml), and 10% fetal bovine serum. Below mentioned procedure was followed for the sub culturing.

1. Culture medium from the cell culture flask was removed.
2. Trypsin-EDTA solution (2 ml) was added to flask and was shaken to allow the detachment of the cells.
3. Cells were observed under the inverted microscope until cell layer was dispersed (usually within 5 min).
4. Complete medium (2 ml) was added to cell dispersion to neutralise trypsin and then centrifuged at 2000 rpm for 3 min.
5. Pellet of cells was resuspended in minimum volume of complete growth medium.
6. Cell culture was (10^5 Cells) then added to cell culture flask and 10 ml of complete growth medium was added to it.
7. Culture was incubated at 37 °C, 5% CO_2.
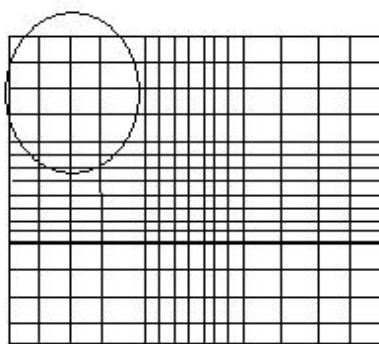
FIGURE 4 1. Cell Counting Using Haemocytometer

A. Preparing Haemocytometer

1. Haemocytometer was cleaned using 70% ethanol.

2. Shoulder of haemocytometer was moistened and a coverslip was affixed using gentle pressure. Newton's ring formation was observed indicating correctly affixed coverslip which ensures correct depth of the chamber.

B. Preparing Cell Suspension

1. Cells were detached from cell culture flask as mentioned above and then suspended in small volume of medium

2. Homogeneous cell suspension was prepared by gentle shaking.

3. Prepared suspension was mixed with equal volume of trypan blue.

C. Counting

1. Small quantity of cell suspension with trypan blue was carefully filled in the haemocytometer chamber using a micropipette by gently placing tip at the edge of the chamber avoiding overfilling of the chamber. Sample drew out of the pipette through capillary action. Pipette was reloaded and second chamber was filled if required.

2. Focus was set on the 16 corner squares of the haemocytometer (as indicated by a circle in the **2** below) using 10X objective of the microscope.
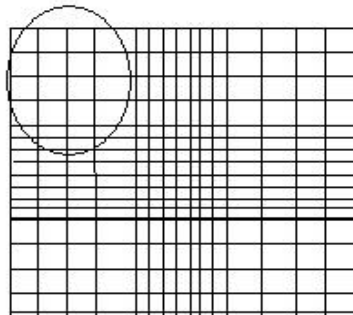
FIGURE 4 2. Haemocytometer diagram for cell counting.

3. Number of cells in the 16 square area of haemocytometer was counted using a hand tally counter. Dead cells stained blue by trypan blue were excluded from counting. All live cells within the area and those positioned on the right and bottom edge of 16 squares outer grid were counted while those on left and upper edge (outer edge of haemocytometer chamber) were excluded.

4. Viable cell count was performed on the on all 4 sets of 16 squares at each corner of haemocytometer.

5. Number of cells in one set of 16 corner squares is equivalent to the number of cells in that set x 10^4 /mL.

6. Average number of cells in all 4 sets of 16-square corners was calculated using following equation.

The total count from 4 sets of 16 corners = Average no. of cells/mL x 10^4 x 2

Where 10^4 is conversion factor (conversion of 0.1 mm^3 to ml) and 2 is dilution factor.

4.2. In Vitro Cytotoxicity Assay (MTT Assay)

This is a colorimetric assay that measures the reduction of yellow 3-(4,5-dimethythiazol-2-yl)2,5-diphenyl tetrazolium bromide (MTT) by mitochondrial succinate dehydrogenase. The MTT enters the cells and passes into the mitochondria where it is reduced to an insoluble, coloured (dark purple) formazan product. The cells are then solubilized with an organic solvent (eg. isopropanol) and the released, solubilized formazan reagent is measured spectrophotometrically. Since reduction of MTT can only occur in metabolically active cells the level of activity is a measure of the viability of the cells. Tetrazolium dye reduction is dependent on NAD(P)H dependent oxidoreductase enzymes largely in the cytosolic compartment of the cell. Therefore, reduction of MTT and other tetrazolium dyes increases with cellular metabolic activity due to elevated NAD(P)H flux. Resting cells such as thymocytes and splenocytes that are viable but metabolically quiet reduce very little MTT. In contrast, rapidly dividing cells exhibit high rates of MTT reduction. It is important to keep in mind that assay conditions can alter metabolic activity and thus tetrazolium dye reduction without affecting cell viability and that different tetrazolium dyes will give different results depending on whether they are reduced intracellularly (MTT, MTS) or extracellularly (WST-1)[1, 2].

Method

The cytotoxicity of gemcitabine carriers were determined using 3-(4, 5-dimethylthiazole-2-yl)-2,5- diphenyl tetrazolium bromide (MTT; Himedia, India) assays. A549 was seeded onto 96-well plates at a density of 5×10^3 cells/well. After 24 h, cells were treated separately with CLs, PLs and RGD-grafted liposomes (at concentrations of gemcitabine 0.01μM, 0.1μM, 1μM and 10μM) were added to wells) in DMEM media containing 10% FBS and antibiotics.

In all wells, after 6 hr transfection media was replaced by fresh DMEM containing 10% of FBS and antibiotics. The cells were incubated for 48 hr, and then 20 μL of 5 mg/mL MTT solution was added to each well. After incubating for 4 hr with MTT solution, the culture medium was

removed and 200 μL of a dimethyl sulfoxide (DMSO) (Sigma, USA) was added. The reduction of viable cells was measured by calorimetry at 570 nm wavelength using an enzyme-linked immunosorbent assay (ELISA) plate reader (Bio-Rad, USA). Cell viability of each group was expressed as a relative percentage to that of control cells. Cells treated with PBS (Phosphate buffer saline) were considered as negative control.

4.2.1. Results and Discussion
4.2.1.1. In Vitro Cytotoxicity Assay (MTT Assay)
The antitumor activity of the novel pharmaceutical preparations containing four different concentrations of gemcitabine (0.01, 0.1, 1 and 10 μM) were compared with free drug against A549 cell lines **(Table 4.1 & Figure 4.3)**. All formulations resulted in concentration dependent inhibition of the proliferation of A549. The lowest cell viability, i.e. the highest cell mortality, appeared at the highest concentration of the liposomal formulations, which proves the controlled and sustained efficacy of the liposomal formulation. Furthermore, the liposomal formulations prevent the toxic effect of the drug applied at high concentration of drugs and thus can increase the maximum tolerance dose (MTD). It is clear from the results that the PLs and RGD grafted liposomes demonstrated higher cytotoxicity than the free drug formulation at the same drug concentration and exposure time, which means that for the same therapeutic effect, the drug needed for the PLs and RGD grafted liposomal formulation could be much less than that for the free drug. Therefore, the development of the PLs and RGD grafted liposomes thus can enhance the therapeutic effect of gemcitabine. *In vitro* cell line studies for the cytotoxicity of prepared nano-constructs were thoroughly carried out. From the results of MTT assay, it was seen that PLs and RGD grafted liposomes were significantly ($p < 0.05$) less toxic than free drug.

TABLE 4 1. Viability of A549 Cells on Exposure to Liposomes

Formulations		% Cell Viability			
		Gemcitabine concentration			
		0.01μM	0.1μM	1μM	10μM
Free Drug	Mean	98.25	85.04	58.88	32.54
	SEM	2.11	1.25	2.01	1.78
CLs liposomes	Mean	90.05	78.20	51.20	30.52
	SEM	1.14	2.04	2.18	2.09
PLs liposomes	Mean	85.21	55.25	32.25	18.25
	SEM	1.75	2.24	2.85	1.96
RGD-grafted liposomes (3%)	Mean	83.11	57.25	35.27	21.05
	SEM	1.29	1.57	2.27	1.82
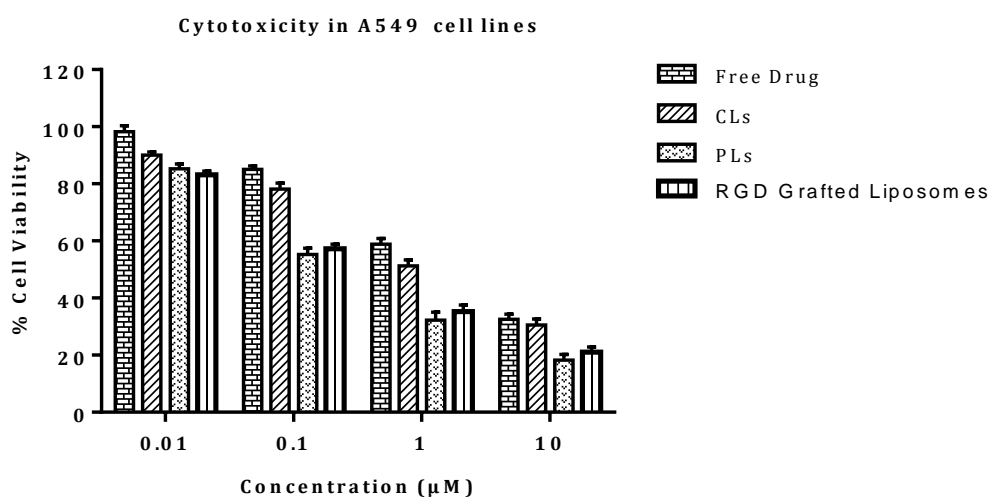
FIGURE 4 3. Cytotoxicity of Different Liposomes in A549 Cell-line.

Various *in vitro* cell line studies were carried out for further screening of prepared liposomal carriers to achieve maximum gemcitabine uptake inside the cells with desired transfection.

4.3 In vitro Cell Uptake Studies

4.3.1 Preparation of Rhodimine loaded liposomes

The rhodamine loaded CLs, PLs, and RGD grafted liposomes were prepared as described in previous chapters by just replacing GEM with 10μM of Rhodamine. The lipid concentrations and other process and formulation parameters were kept similar to the preparation of optimized GEM loaded CLs and RGD grafted liposomes. The prepared rhodamine loaded

liposomes were stored in amber coloured vials, covered with aluminium foil, at 2-8 ^{0}C. This was used for the cellular uptake studies. Flow cytometry was utilized for quantitative cell uptake to determine the mean fluorescent intensity while qualitative intracellular accumulation was determined using confocal microscopy.

4.3.2 Flow Cytometry

Since the first application of flow cytometry (FCy) in the 1970s [3], the machines have become widely popular in research and clinical diagnostics. In principle, FCy can be combined with nearly any staining procedure, assay or biotechnological process. Whenever fluorescence is introduced into a microorganism or a cell it can be exploited in flow cytometry for assessing information about the specimen. To a low extent the technology is applied for other objects than microorganisms and cells [4]. But with the combination of fluidics and laser triggered fluorescence detection it is the ideal tool to detect NPs in cells. Subtle changes in scattering and emission of a cell can be observed – which are directly linked to the cellular uptake of fluorescing particles.

In flow cytometry, a fluidics system is coupled with the detection of fluorescence and of light scattering in small and wide angle position. For this application the objects of interest must be prepared as a diluted dispersion commonly not exceeding a concentration of several thousand objects per µl. In the machine, a sample stream is injected into the core of a flowing stream of so called sheath liquid (water or physiological buffer) and a laminar flow is established. The two streams do not mix and the sample flow is surrounded by a layer of sheath liquid flow in a concentric setup. This is termed hydrodynamic focusing. This stream of two concentric layers is directed through the measurement chamber, a narrow glass capillary. In the measurement chamber, the sample stream is hit orthogonally by a laser beam. It is important to note that the objects, e.g. cells, pass this laser beam single-filed. Placed behind an array of filters and mirrors, several detectors successively detect the properties of each cell passing the laser beam. This includes fluorescence signals but also of wide angle (sideward scatter, SSC) and small angle (forward scatter, FSC) scattering. Flow cytometers thus allow for the rapid measuring of individual objects in dispersion. Another obvious advantage is the short exposure of each object to the laser (µs scale), unlike e.g. in microscopy where exposure lasts seconds to minutes. Extremely light sensitive objects can be analyzed by flow cytometry. Within one second, several thousand objects can be measured separately and their number per volume can be counted. But only when one object passes through the beam of the reference laser, data acquisition is triggered. In this instant, a digital event is created and the acquired data from every active channel is assigned to this event i.e. assigned to this particular object. Each event now represents a comprehensive data

set, including fluorescence intensities in various channels and scattering intensities at two fixed positions (small and large angle i.e. FSC and SSC). This collected raw data consists of up to hundred thousands of events which represent background (e.g. pieces of cell debris) and wanted objects (cells) alike. Before final data interpretation the signals must be sorted from the background events. Fluorescence, granularity (SSC) or the presumable size (FSC or SSC) are features which can be applied to identify the wanted objects. Commonly a threshold condition is set on one of the detection channels so that unwanted signals are excluded from detection. In nearly every system a 488 nm laser is present as standard reference, but often additional lasers (e.g. 640 nm, 561 nm, 375 nm) are available.

Method

A549 cells were seeded at a density of 5×10^5 cells per well in 24 well plates. After 24 hr of proliferation, formulations (**Table 4.2 & 4.3**) containing Rhodamine at a final concentration of 10 µM were exposed to cells and incubated for additional 6 hr at 37^0C in humidified air with 5% CO_2. After incubation, the cells were harvested and washed three times with cold PBS having pH = 7.4 and then analysed for mean fluorescence activity using fluorescence activated cell sorter (FACS-BD-AriaIII, BD, USA).

TABLE 4 2. Cell-Line Treatment Parameters for Flow-Cytometry

Sr.No.	Formulations	Cells	Treatment	Condition
1	CLs liposomes			
3	RGD-grafted liposomes (1%)			
3	RGD- grafted liposomes (3%)	A549	10 µM Rhodamine liposomes	Incubation time=48 h Temperature = 37°C (5% CO_2)
4	RGD- grafted liposomes (5%)			

4.3.3 Confocal Microscopy

Cellular internalization of Rhodamine liposomes in A549 cells was monitored by confocal microscopy.

Method

Cells were seeded onto 6-well plates with a glass cover slip at the bottom. Cells were seeded at a density of 10^4 cells/well on flame sterilized 0.17 mm square glass cover slips in a 6 well plate. After 24 hr of seeding, cells were transfected with Rhodamine liposomes containing

formulation (**Table 4.4**) at a final concentration of 10 µM. After 6 hr of incubation, cells were washed with cold PBS immediately and fixed using ice cooled 4% paraformaldehyde solution for 10 min. Cells were stained by cell nuclei stain, DAPI, for next 10 min. Cover slips were mounted on slides after washing with PBS three times and proceeded for confocal microscopy using confocal laser scanning microscope (LSM 710, Carl-Zeiss Inc., USA).

TABLE 4 3. Cell-Line Treatment Parameters for Confocal Microscopy

Sr.No.	Formulations	Cells	Treatment	Condition
1.	CLs liposomes	A549	10 µM Rhodamine liposomes	Incubation time= 6 h Temperature = 37°C (5% CO_2)
2.	RGD-grafted liposomes (3%)			

Live imaging was performed using confocal microscopy to access the potential of RGD grafting on the liposomal surface. Live imaging was carried out in A549 cells using three formulations, i.e. CLs liposome, PLs liposomes and RGD-grafted liposomes.

$5x10^4$ cells were seeded onto confocal microscopic petridish with glass cover slip (Nunc, India). After 24 hr cells were transfected with Rhodamine liposomes at 10 µM concentration. Soon after transfection imaging was started. Furthermore, the lateral Z-stack images were constructed during imaging from the middle zone of the cells.

4.3.4 Sub-inhibitory concentration (Cell Cycle Analysis)

Cellular growth is considered as successive phases, characterized by specific biochemical processes and called, from one division to the other: 'cell cycle' [5]. Each cell has to replicate its genetic material during the DNA synthesis phase (S phase) before entering the mitotic phase (M). Moreover, periods of time (gaps) are located between the end of cellular division and DNA synthesis start (G 1 phase) as well as between the end of DNA synthesis and mitosis start (G 2 phase). The mitotic phase is distinguished from other cycle phases (called together interphase). To reach the mitotic phase, cells have to double their whole components, at the same time that their genetic material doubles. Constituent synthesis is generally continuous, with a varying rate during interphase[6]. The growth cycle is considered as distinct from the nuclear cycle and its regulation mechanism seems to be different[7], but these two cycles are closely dependent and have to converge in a synchronous way towards mitosis; otherwise, there is an unbalanced growth[8]. DNA amount in cells is often the single parameter measured for cell cycle studies by flow cytometry. Analyses are performed with fluorescent molecules that bind specifically and stoichiometrically to DNA, in order to obtain a linear relationship between cellular fluorescence intensity and DNA amount[9]. Some dyes possess

an intercalative binding mode, such as propidium iodide or ethidium bromide, whereas others present an affinity for DNA A-T rich regions: Hoechst 33342, Hoechst 33258 and DAPI, or G-C rich regions: mithramycin and chromomycin A3.

Method

Chemosensitization is well governed at sub-inhibitory concentration and hence, cell cycle analysis was used to determine the DNA content of cells at varying concentration of RRM1 siRNA i.e. 50 pM, 100 pM, 500 pM and 2.5 nM. RGD-grafted liposomes only were used to find out the optimal concentration which regulates sub-inhibitory growth of cancer cells in both A549 and H1299 cell lines. Cells were seeded onto 6-well plates at a density of 10^6 cells/well. After 24 hr of seeding, cells were transfected with RRM1 siRNA containing RGD-grafted liposomes at varying siRNA concentrations in DMEM media containing 10 % FBS and antibiotics.

In all wells, after 6 hr transfection media was replaced by fresh DMEM containing 10% of FBS and antibiotics. The cells were incubated for 72 hr and then washed with PBS thrice. 10^6 cells were suspended in 1mL of PBS and vortexed gently to obtain a mono-dispersed cell suspension, with minimal cell aggregation. Cells were centrifuged at 200 x g for 5 min at room temperature and again re-suspended in 0.5 mL of PBS. Cells were fixed by transferring this suspension into centrifuge tubes containing 4.5 mL of 70 % ethanol, on ice. Cells were kept in above step for at least 2 h at 4°C. Above ethanolic suspension was centrifuged for 5 min at 300 x g and ethanol was decanted thoroughly. Again cells were suspended in 5 mL of PBS and centrifuged at 300 x g for 5 min. Finally cell pellet was re-suspended in 1 mL of PI staining solution and kept in the dark at room temperature for 30 min. Samples were transferred to the flow cytometer and cell fluorescence was measured. Maximum excitation of PI bound to DNA was at 536 nm, and emission was at 617 nm. Blue (488 nm) or green light lines of lasers were optimal for excitation of PI fluorescence.

4.4 Results and Discussion

4.4.1. In vitro cell uptake

4.4.1.1 Flow Cytometry

RGD was attached on the cell surface to enhance the gemcitabine uptake inside the cells. Initially, the liposomal formulations, CLs liposomes was studied by grafting 1%, 3% and 5 mole% RGD on the liposomal surface. 3 mole % of RGD was found to be optimal. 3 mole% RGD incorporation showed significantly higher amount of cell uptake as compared to 1 mole% of RGD, while 5 mole% did not show further enhancement in cell

uptake (**Figure 4.4)** and hence, RGD-grafted liposomes (3%) was selected for further studies.

TABLE 4 4 Uptake of Liposomes in A549 Cells

Formulations	MFI	
	Mean	**SEM**
RGD-grafted liposomes (1%)	82.08	1.34
RGD-grafted liposomes (3%)	85.15	1.22
RGD-grafted liposomes (5%)	86.85	1.57

Cell uptake in A549 cell line
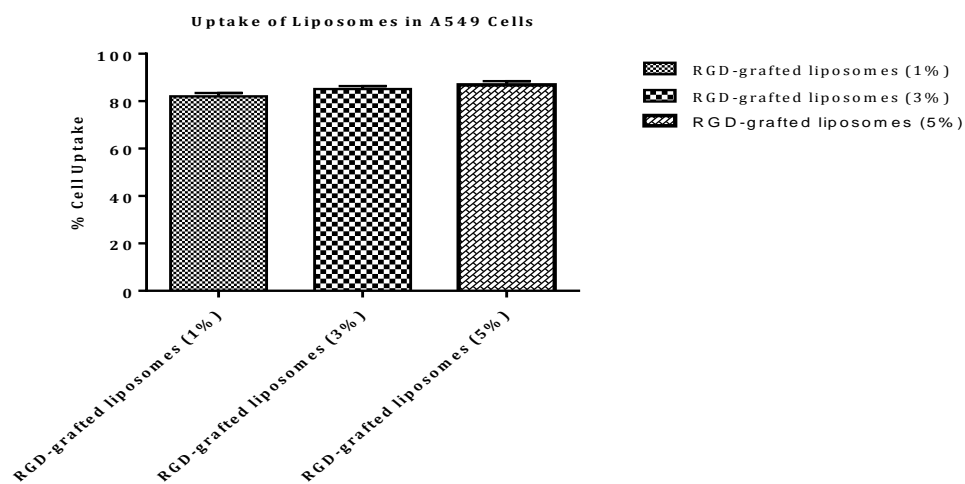
FIGURE 4 4 Uptake of Liposomes in A549 Cells

As shown in **Figure 4.5** and **Figure 4.6**, the order of fluorescence intensity in cells after treatment with various GEM formulations was as follows: in A549 cell line: CLs liposomes < RGD-grafted liposomes

It was suggested from these results that nano-constructs could significantly enhance gemcitabine translocation into cells. The CLs liposomes showed enhanced mean fluorescent intensity by grafting 3mol% of RGD peptide on the liposomal surface. Furthermore, RGD-grafted liposomes showed significantly more MFI inside the cells (A549).

CLs Liposomes   **RGD grafted Liposomes**
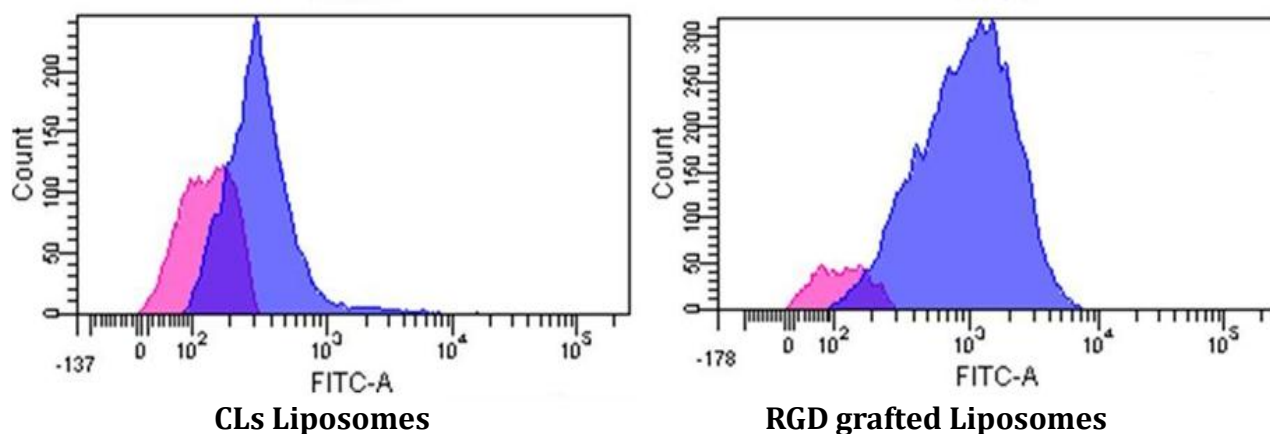
FIGURE 4 5. Quantification of Mean Fluorescence Intensity in A549 Cells

Formulations	MFI	
	Mean	**SEM**
CLs liposomes	66.08	1.34
RGD-grafted liposomes (3%)	85.15	1.22
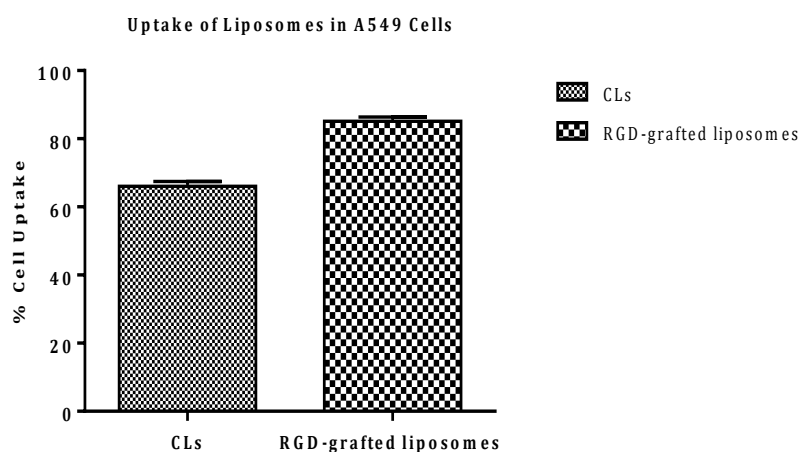
FIGURE 4 6. Uptake of Liposomes in A549 Cells

The lipids used in the formulation provided sufficient strength to retain gemcitabine in liposomal environment and RGD grafting shows significant enhancement in cell uptake in cell lines compared to the CLs. Both, quantitative and qualitative, techniques support this hypothesis.

4.4.1.2 Confocal studies

Results from flow cytometry were well supported by qualitative analysis where intracellular localization of Rhodamine liposomes (Red) was investigated using laser confocal microscope as shown in **Figure 4.7 and Figure 4.8**. After 6 hr incubation, Rhodamine liposomes was mainly observed in cytoplasm with a relative uniform distribution. Confocal microscopy also showed that RGD grafting helps to enhance the cellular localization in cell lines.
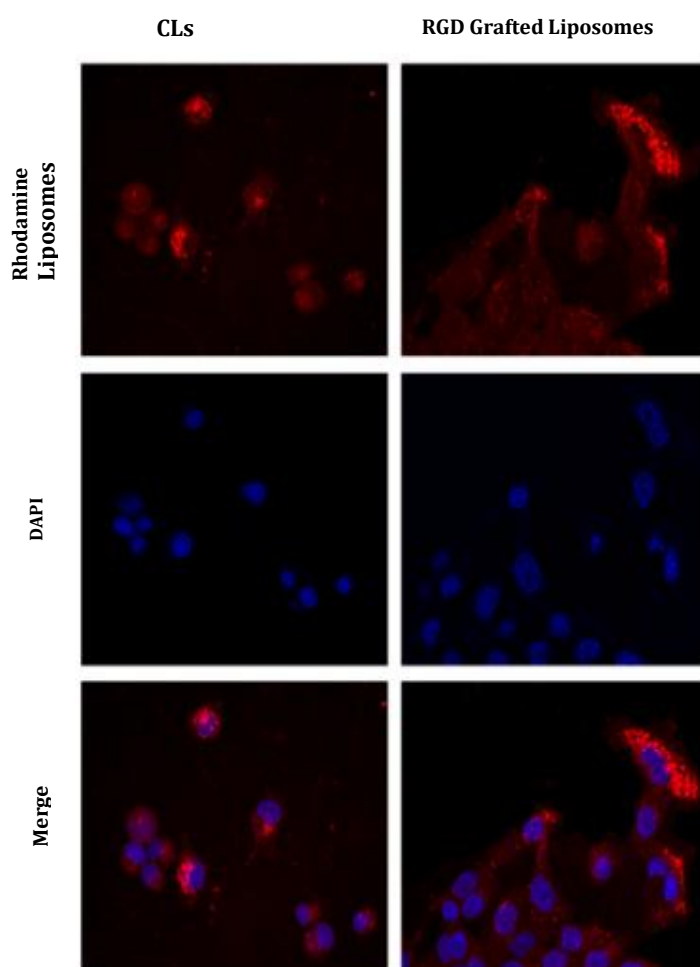
FIGURE 4 7. Cell Uptake in A549 Cell Line

To investigate the mechanism or pattern of uptake by the mean of RGD grafting, live uptake was monitored for CLs liposomes and RGD-grafted liposomes by Z-stacking.

Z-stack images (**Figure 4.9 and Figure 4.10**) revealed CLs liposomes get accumulated inside the liposomes soon after transfection but RGD-grafted liposomes showed different pattern for uptake. They initially bound to the cell surface and surface bound liposomes further taken up inside by the mean of phagocytosis. Z-stacking (**Figure 4.9**

and Figure 4.10) showed marginal different pattern of intracellular localization with RGD grafted liposomes as compared to non-grafted formulations.

CLs liposomes helped gemcitabine to get internalized into the cells immediately soon after transfection. GEM was found to localize inside the cell from very beginning and this GEM stayed as such till end. However, at the end after 16 min, flueroscence was found to decrease due to constant exposure of laser. RGD grafted liposomal formulations, RGD-grafted liposomes and initially helped GEM to locate onto the cell surface. However, part of GEM was also internalized as seen with CLs liposomes. After some time GEM translocated from surface to the intracellular region of the cells. These results suggest the receptor based translocation of liposomal GEM inside the cell. This is due to grafting of RGD on the liposomal surface which is detected by the cell surface. RGD have shown to have selective binding affinity against integrin for treatments of human tumor metastasis and tumor-induced angiogenesis. Due to cytoadhesion, cytoinvasion and partial lysosomal accumulation, RGD-mediated drug delivery may provide improved intracellular availability of conjugated liposomal systems [10]. Taken collectively, live imaging with Z stack at different time points confirmed that GEM is not localized to the apical surface of the cells; rather it travelled through the cell membrane inside the cell and thus reveals the targeting potency of RGD towards cancer cells.
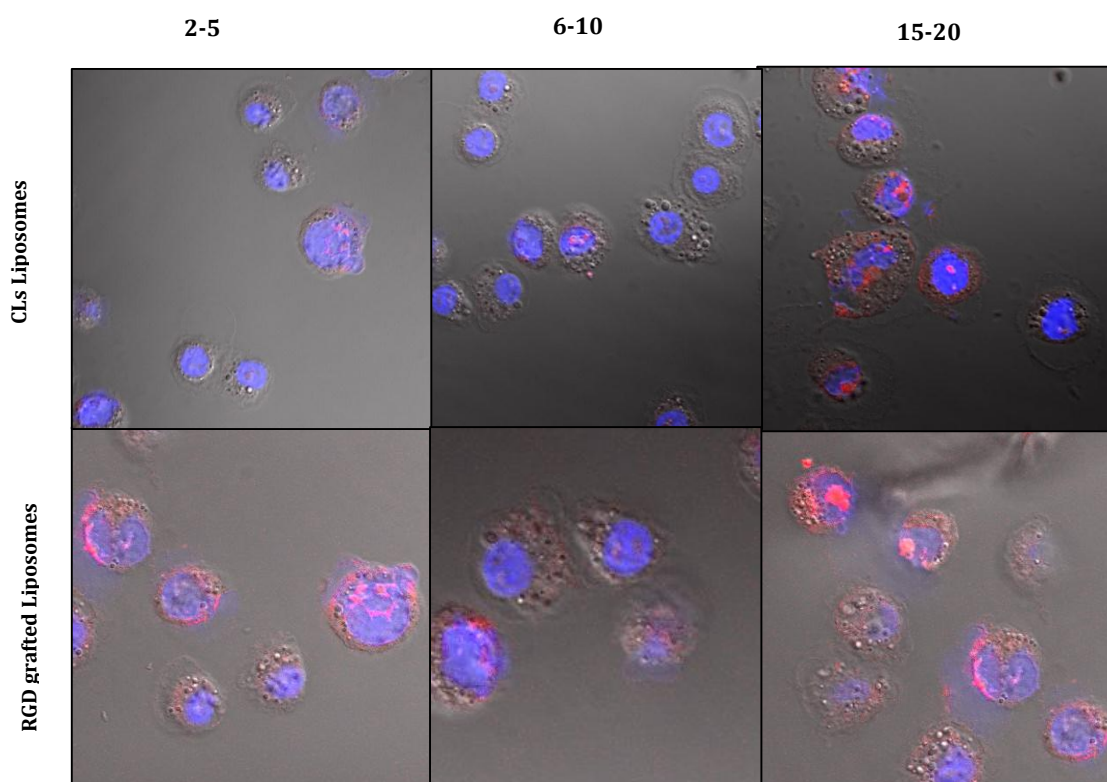
FIGURE 4 8. Live uptake of CLs and RGD grafted liposomes in A549 cells
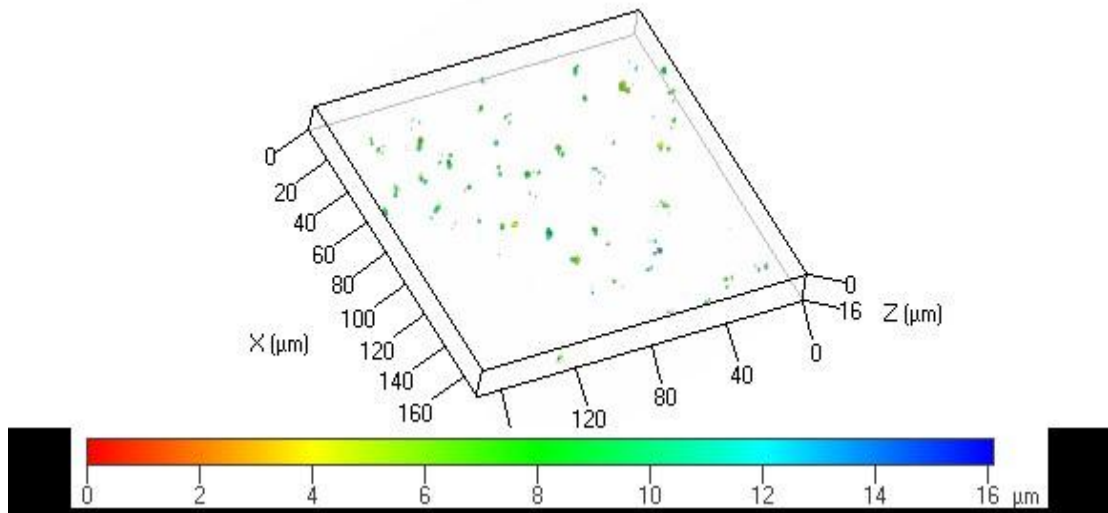
FIGURE 4 9. 3D Z-stack image for CLs liposomes uptake
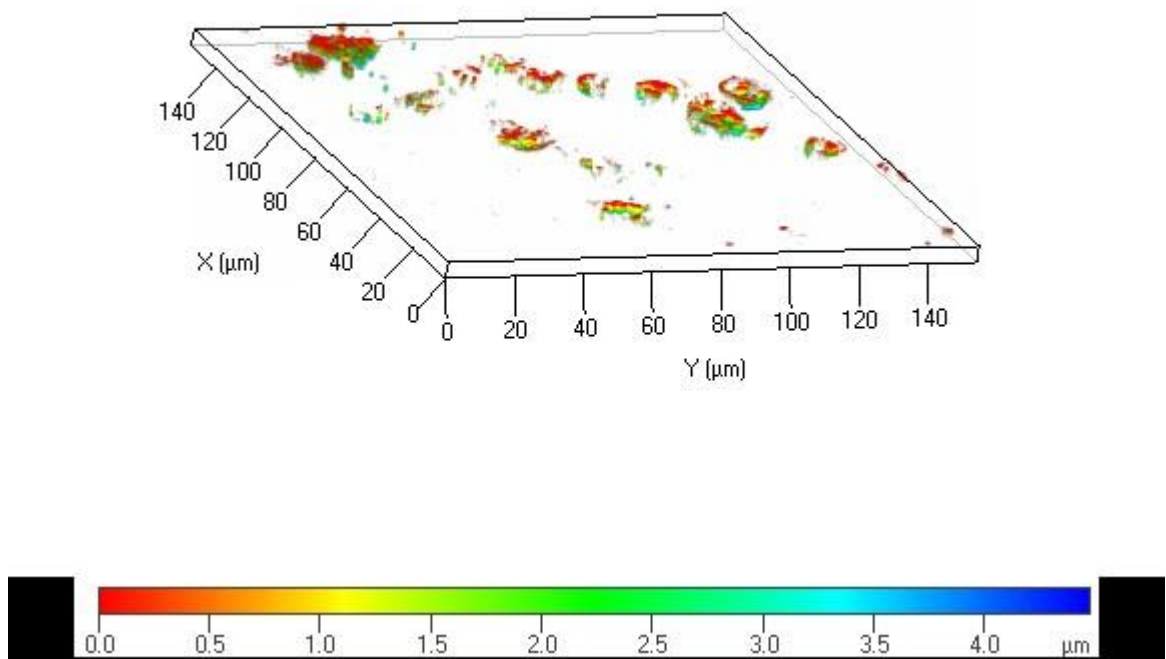
FIGURE 4 10. 3D Z-stack Image for RGD-Grafted Liposomes Uptake

4.4.1.3. Sub-inhibitory concentration (Cell Cycle Analysis)

Cell cycle analysis revealed that cell growth inhibition occurs at higher concentration i.e. 500 pM and 2.5 nM only (**Figure 4.11** and **Figure 4.12**). However, lower concentrations, 50 pM and 100 pM, did not show any marked inhibition. Both types of cells (A549 and

H1299) showed similar pattern of inhibition. Control siRNA showed no inhibition at 2.5nM concentration.
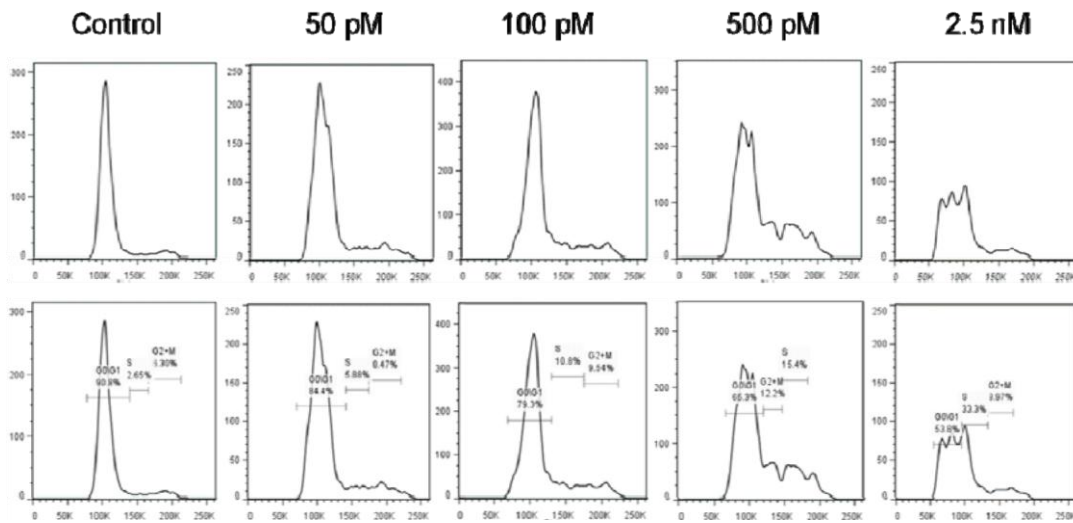
FIGURE 4.11. Cell Growth Inhibition in A549 Cells
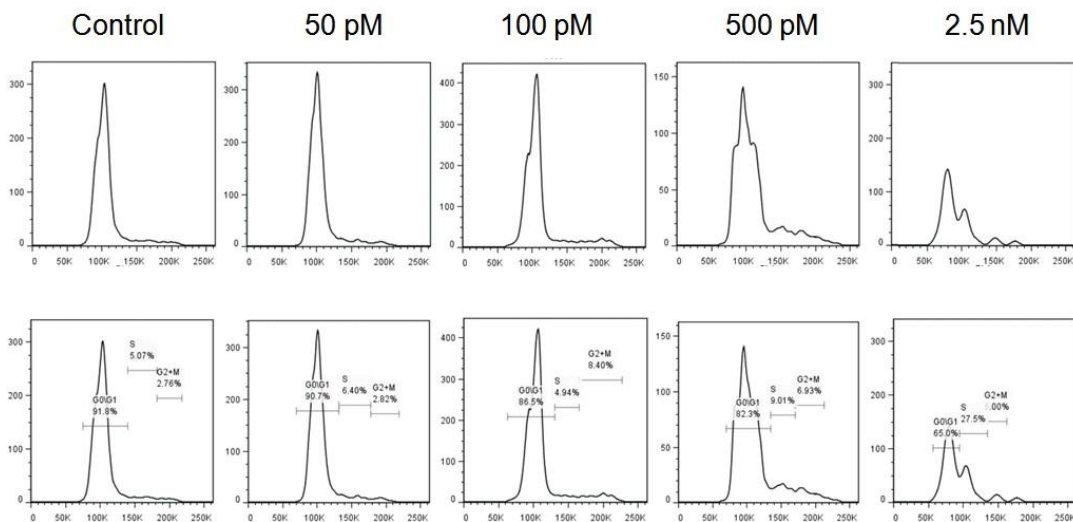
FIGURE 4 11. Cell Growth Inhibition in H1299 Cells

These results suggested that 50 pM of RRM1 siRNA concentration can be taken for chemosensitization. These results can be utilized for further studies to evaluate chemosensitization of a chemotherapeutic drug Gemcitabine HCl because; earlier reports have described the utility of sub inhibitory growth concentration of RRM1 for chemosensitization[11]. Further, this fact was reassessed using transfection study by the mean of gene knock down effect and that study also supported the results obtained from cell cycle analysis. Hence, 50 pM was used for chemosensitization of cancer cells for further studies.

4.5. Chemosensitization Studies

Although a number of chemotherapeutic treatments have been shown to be effective at inhibiting or eliminating cancer cell growth in preclinical studies, clinical applications are often limited due to the toxic side effects associated with anticancer drugs. Patients are often unable to tolerate the level of a drug needed to effectively eliminate malignant cells while levels that can be tolerated are insufficient therapeutically. As a result, chemo-resistance and subsequent tumor recurrence are often the outcome of such therapies. An example of this all too common event is the use of taxanes (paclitaxel and its semi-synthetic analogue, docetaxel) in the treatment of a variety of cancers including ovarian, breast, prostate, and non-small cell lung cancers [12, 13]. While surgery along with taxane- and platinum-based chemotherapy for advanced ovarian cancer has allowed up to 80% of women to achieve a clinical response[14], cancers in most patients initially diagnosed with late stage disease eventually recur. Development of methods to circumvent resistance may ultimately improve the impact of adjuvant therapy, resulting in prolonged disease-free intervals and survival. Novel targeted therapies that interfere with specific molecular signalling pathways affecting cancer cell survival are being developed as potential treatment options to render cancer cells more sensitive to cytotoxic chemotherapy. Targeted therapies that increase cancer cell sensitivity to chemotherapies offer the benefits of lowering unwanted side effects and increasing the likelihood of destroying resistant cells while avoiding healthy cells where there is little or no expression of the targeted entity.

Method

In vitro cytotoxicity of anticancer drug Gemcitabine HCl at sequential concentrations was assessed with pre-treatment of RGD grafted siRNA nano-constructs (RGD-DDHC liposomes and RGD-CPE liposomes) in A549 and H1299 cells. All the siRNA formulations were obtained by Nirav Khatri and Ambikanadan Misra, Pharmacy dept., The M. S. University of Baroda. Gemcitabine HCl solution (Gem. sol.) and Gemcitabine HCl liposomes (Gem. lipo.) were used as chemotherapeutic agents. Gemcitabine solution was obtained by reconstituting lyophilized injection of Gemcitabine HCl (Gemtaz, Sun Pharma Ind. Ltd., India) with saline solution. Lyophilized injection was composed of Gemcitabine HCl, liposomes were made up of DPPC, DSPG, cholesterol, mPEGDSPE$_{2000}$ (5.6: 2: 2: 0.4) with mean particle size of 150 nm. Entrapment efficiency of prepared liposomes was 60.6±4.32%.

Aliquots of 10^6 cells were seeded in 60 mm petri dishes. After 24 hr proliferation, the cells were transfected with RRM1 siRNA containing RGD-DDHC liposomes and RGD-CPE liposomes in antibiotics and serum free medium. The final concentration of RRM1 siRNA was 50 pM. After 6 hr transfection, the culture medium was replaced with fresh DMEM supplemented with 10% FBS and antibiotics. Following next 42 hr of incubation, cells were harvested and seeded in 96-well plates at a density of 5×10^3 cells per well. After 24 hr proliferation, cells were treated with a series of concentrations of Gemcitabine solution or Gemcitabine liposomes for 48 hr, and 20 µl of a 5 mg/ml MTT was added to detect IC_{50} values. Along with these sets of experiments, sets of samples without pre-exposure to RRM1 siRNA were also investigated and IC_{50} values were determined.

4.5.1. Result and Discussion

MTT assay was used to determine IC_{50} values of Gemcitabine HCl in A549 and H1299 cells pre-treated with RGD grafted siRNA nano-constructs at final RRM1 siRNA concentration of 50 pM in both cell lines. Cell viability was accessed in a range of Gemcitabine HCl concentration i.e. 0.005 nM to 250 nM. Cell viability at these concentrations after 48 hr with and without pre-exposure to RRM1 siRNA by the mean of RGD-DDHC liposomes, RGDCPE liposomes is given in **Table 4.5** and **Table 4.6** Viability of A549 and H1299 Cells on exposure of various formulations is graphically represented in **Figure 4.13** and **Figure 4.14**.

H1299 cell line showed more amount of viable cells after 48 hr as compared to A549 cells. In both types of cells, Gem. sol. (without pre-exposure to RRM1 siRNA) showed highest IC_{50} values of 6.28 ± 0.37 and 19.26 ± 1.07 in A549 and H1299 cells, respectively. The order of IC50 values for Gemcitabine HCl in both A549 and H1299 cells were as follow (**Table 4.7**):
Gem. sol. < Gem. lipo. < RGD-CPE liposomes+Gem. sol. < RGD-DDHC liposomes+Gem. sol. < RGD-CPE liposoes+Gem. lipo. < RGD-DDHC liposomes+Gem. lipo

siRNA pre-treated Gemcitabine liposomes and siRNA pre-treated Gemcitabine solution exposed cells showed significantly less IC_{50} values as compared to IC_{50} values of cells treated with Gemcitabine liposomes and Gemcitabine solution alone. Results strongly suggest the chemosensitization effect by pre-exposure of siRNA in liposomal forms at picomolar concentration (**Table 4.8, Table 4.9** and **Table 4.10**).

TABLE 4 5. Chemosensitization of Gemcitabine HCl in A549 Cells

Formulation		Gemcitabine Concentration (log nM)									
		-2.30	-1.60	-1.30	-0.60	-0.30	0.40	0.70	1.40	1.70	2.40
RGD-DDHC liposomes(2%)+Gem. lipo.	Mean	98.32	93.39	73.55	60.80	44.45	38.00	33.35	30.95	24.25	22.45
	SEM	2.05	1.92	2.25	1.30	0.85	2.60	1.05	1.95	1.05	0.95
RGD-DDHC liposomes(2%)+Gem. sol.	Mean	101.95	93.61	74.20	63.10	47.20	40.00	38.90	33.20	30.50	29.50
	SEM	1.95	3.29	3.88	5.20	4.00	3.60	3.50	0.90	1.50	2.00
RGD-CPE liposomes(2%)+Gem. Lipo.	Mean	100.39	93.24	74.05	61.35	45.30	39.80	36.10	31.70	26.95	25.85
	SEM	0.01	1.76	1.25	1.85	1.70	0.80	0.60	1.50	1.45	1.55
RGD-CPE liposomes(2%)+Gem. sol	Mean	100.50	94.00	76.30	64.80	48.50	42.30	40.90	34.60	31.40	30.20
	SEM	0.50	3.68	5.98	3.50	5.30	1.30	5.50	0.50	2.40	1.30
Gem. lipo	Mean	102.40	97.05	90.00	80.13	71.05	60.45	57.10	51.85	45.65	41.62
	SEM	1.52	1.65	0.40	0.72	2.35	2.15	1.80	1.65	1.15	2.30
Gem. sol.	Mean	100.78	95.78	88.35	80.02	72.40	68.20	64.60	58.40	50.00	44.42
	SEM	1.08	2.94	5.17	0.52	6.81	7.01	1.40	2.10	2.31	2.79
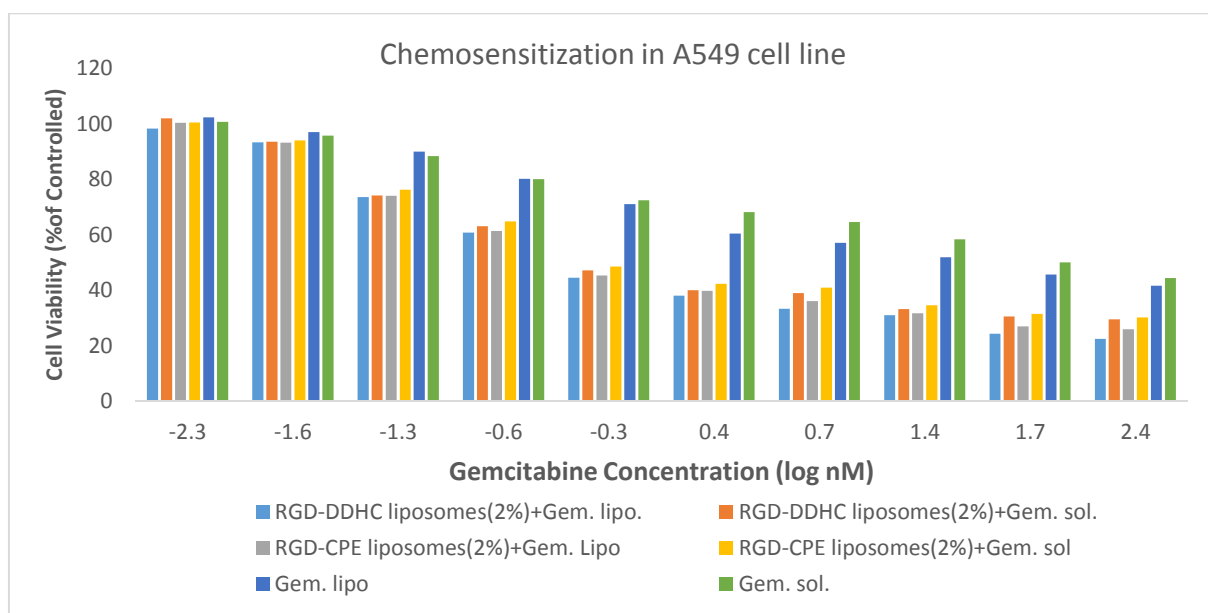
FIGURE 4 12. . Chemosensitization of Gemcitabine in A549 Cells by siRNA

TABLE 4 6. Chemosensitization of Gemcitabine HCl in H1299 Cells

Formulation		Gemcitabine Concentration (log nM)										
		-2.30	-1.60	-1.30	-0.60	-0.30	0.40	0.70	1.40	1.70	2.40	2.70
RGD-DDHC liposomes(2%)+Gem. lipo	Mean	101.34	93.95	87.70	76.90	64.10	62.65	53.25	51.30	46.80	44.50	39.60
	SEM	0.97	1.65	0.30	2.00	1.60	1.45	0.15	1.10	1.00	0.30	1.60
RGD-DDHC liposomes(2%)+Gem. sol.	Mean	101.40	99.00	87.30	80.30	68.70	60.90	55.60	52.10	50.50	43.80	41.50
	SEM	1.40	3.40	1.60	2.80	2.10	0.80	2.70	2.90	2.90	1.50	0.60
RGD-CPE liposomes(2%)+Gem. lipo.	Mean	100.39	93.65	88.80	77.05	67.90	62.50	55.05	51.31	45.60	43.05	39.50
	SEM	0.01	1.35	1.40	1.25	2.20	1.60	1.65	1.09	1.10	0.95	1.00
RGD-CPE liposomes(2%)+Gem. sol.	Mean	99.70	95.60	92.30	78.40	70.90	63.90	55.70	54.60	46.10	43.90	40.90
	SEM	0.30	1.60	1.10	2.10	2.00	1.70	0.40	2.00	0.10	0.80	2.50
Gem. lipo.	Mean	100.19	96.85	91.35	85.85	77.95	74.10	71.45	66.55	61.15	48.90	45.15
	SEM	0.69	1.85	0.95	0.55	1.55	1.10	1.15	1.25	0.85	1.70	1.15
Gem. sol.	Mean	99.00	98.30	94.20	84.20	80.30	76.90	74.20	68.90	61.40	57.90	46.30
	SEM	0.30	1.60	2.20	2.20	3.70	2.00	2.10	3.10	1.90	3.00	2.00

Chemosensitization in H1299 cell line
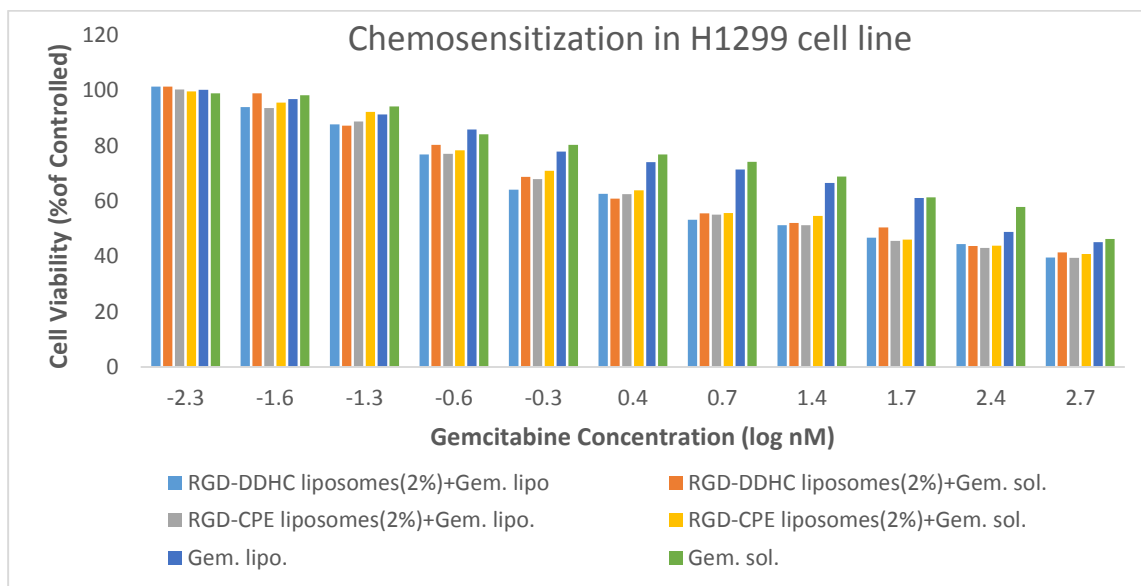
FIGURE 4 13. Chemosensitization of Gemcitabine in H1299 Cells by siRNA

TABLE 4 7. IC$_{50}$ values of Various Formulations with or without siRNA

Sr.No.	Formulation	IC$_{50}$	
		A549	H1299
1.	RGD-DDHC liposomes(2%)+Gem. lipo	1.23±0.12	4.42±0.28
2.	RGD-DDHC liposomes(2%)+Gem. sol.	1.35±0.56	4.97±0.19
3.	RGD-CPE liposomes(2%)+Gem. lipo.	1.27±0.10	4.59±0.46
4.	RGD-CPE liposomes(2%)+Gem. sol.	1.53±0.12	5.30±0.51
5.	Gem. lipo.	3.93±0.25	12.50±0.93
6.	Gem. sol.	6.28±0.37	19.26±1.07

Chemosensitization effect is described by the fold change in IC$_{50}$ values when siRNA was preexposed in different formulations. Fold change in IC$_{50}$ values are given in Table 4.8, Table 4.9, Table 4.10 and **Table 4.11**. Highest chemosensitization (fold change=5.11) was observed in cells pre-treated with RGD-DDHC liposomes followed by treatment with Gem. lipo. as compared to treatment with Gem. sol. alone. The order of fold change in IC$_{50}$ values for RGDDDHC liposomes and no significant difference was observed between RGD-CPE-liposomes.

TABLE 4 8. Change in IC_{50} of Gemcitabine HCl after Chemosensitization by RGD-DDHC Liposomes(2%)

Sr.No.	Fold change in IC_{50}		
	RRM1 siRNA Pre-exposure with RGD-DDHC liposomes(2%)	A549	H1299
1.	Gem. sol./RGD-DDHC liposomes(2%)-Gem. lipo.	5.11	4.36
2.	Gem. sol./RGD-DDHC liposomes(2%)-Gem. sol.	4.65	3.88
3.	Gem. lipo./RGD-DDHC liposomes(2%)-Gem. lipo.	3.20	2.83
4.	Gem. lipo./RGD-DDHC liposomes(2%)-Gem. sol.	2.91	2.52

TABLE 4 9. Change in IC_{50} of Gemcitabine HCl After Chemosensitization by RGD-CPE Liposomes(2%)

Sr.No.	Fold change in IC_{50}		
	RRM1 siRNA Pre-exposure with RGD-CPE liposomes(2%)	A549	H1299
1.	Gem. sol./RGD-CPE liposomes(2%)Gem. lipo.	4.94	4.20
2.	Gem. sol./RGD-CPE liposomes(2%)Gem. sol.	4.10	3.63
3.	Gem. lipo./RGD-CPE liposomes(2%)Gem. lipo.	3.09	2.72
4.	Gem. lipo./RGD-CPE liposomes(2%)Gem. sol.	2.57	2.45

Fold change of 1.10 & 1.12, 1.20 & 1.15 and 1.09 & 1.09 was observed for RGD-DDHC liposomes(2%)- Gem. sol./ RGD-DDHC liposomes(2%)-Gem. lipo., RGD-CPE liposomes(2%)-Gem. sol./ RGD-CPE liposomes(2%)-Gem. lipo. and respectively, as compared to 1.60 & 1.54 for Gem. sol./Gem. lipo. By comparing the fold change in IC_{50} values of Gem. sol. vs Gem. lipo. in with and without pre-exposure for in all formulations, it can be said that pre-exposure of siRNA has dominating effect in fold change as compared to liposomal vs solution form. However, one should not neglect the beneficial effect of liposomal for over simple solution.

TABLE 4 10. Comparison of Change in IC_{50} Value of Various Formulation

	Fold change in IC_{50}

Sr.No.	Gem. Sol. vs Gem. lipo.	A549	H1299
1.	Gem. sol./Gem. lipo.	1.60	1.54
2.	RGD-DDHC liposomes(2%)- Gem. sol./ RGD-DDHC liposomes(2%)-Gem. lipo.	1.10	1.12
3.	RGD-CPE liposomes(2%)- Gem. sol./ RGD-CPE liposomes(2%)-Gem. lipo.	1.20	1.15

The 5-fold increase in Gemcitabine sensitivity following sub-growth inhibitory RRM1 knockdown using siRNA nano-constructs correlates well with a previous report [13], where stably expressed shRNAs were used to knockdown RRM1. Additionally, Gemcitabine liposome showed significantly less IC_{50} value ($P < 0.05$) as compared to Gemcitabine solution in both with and without pre-siRNA treatment. This also demonstrates the application of gemcitabine liposome as a substitute for Gemcitabine solution. Due to the higher dose of Gemcitabine HCl, it is very difficult to load sufficient amount of drug inside the liposomes. But, present studies open a vista for chemotherapy at lower dose and at that point it may be possible to formulate clinically suitable liposomes of Gemcitabine HCl with sufficient drug loading. Studies have also demonstrated that transfection with as little as 2.5 nM siRNA caused cell growth inhibition while 50 pM concentrations resulted in a noticeable chemosensitization of the drug Gemcitabine. Taken collectively results suggest that prepared siRNA liposomal formulations may be a novel therapeutic strategy for reducing a dose of Gemcitabine with combination therapy or alone as a chemotherapeutic agent.

4.6. In Vitro Drug Release

The release of GEM from liposomes at various temperatures (25, 30, 37, 40, 42, 45, and 50°C) was determined. Briefly, 20 mg of lyophilized GEM- RGD grafted liposomes was suspended in 1 ml of PBS in a dialysis bag (MWCO:12,000 Daltons) and placed in a screw cap top glass bottle containing 5 ml PBS. It was then heated to a set temperature with gentle and continuous stirring (80 rpm) and maintained for 10 min. After 10 min, amount of GEM released into the receiver medium (PBS) was analyzed using UV spectrophotometer. Total amount of GEM entrapped in liposomes was determined by disrupting them with methanol and diluted to suitable volume with solvent. The percentage release at each temperature was calculated relative to total amount of GEM in disrupted liposomes.

4.6.1 Results & Discussion

Percent release of GEM from RGD grafted liposomes was determined at different temperatures. In general, we observed increase in GEM release (%) with increasing temperature (**Figure 4.15**). However, a sharped increase in GEM release was noticed

between 38°C and 42°C where GEM-liposomes released about 30% of its content. At 42°C, approximately 60% of GEM was released which is statistically significant (**p<0.05) compared with 25% released at 37°C. Release of GEM was fairly constant after 42°C through to 50°C. The release behaviour of GEM liposomes was consistent with studies conducted by Lim and his colleagues [15].

In Vitro GEM Release from liposomes
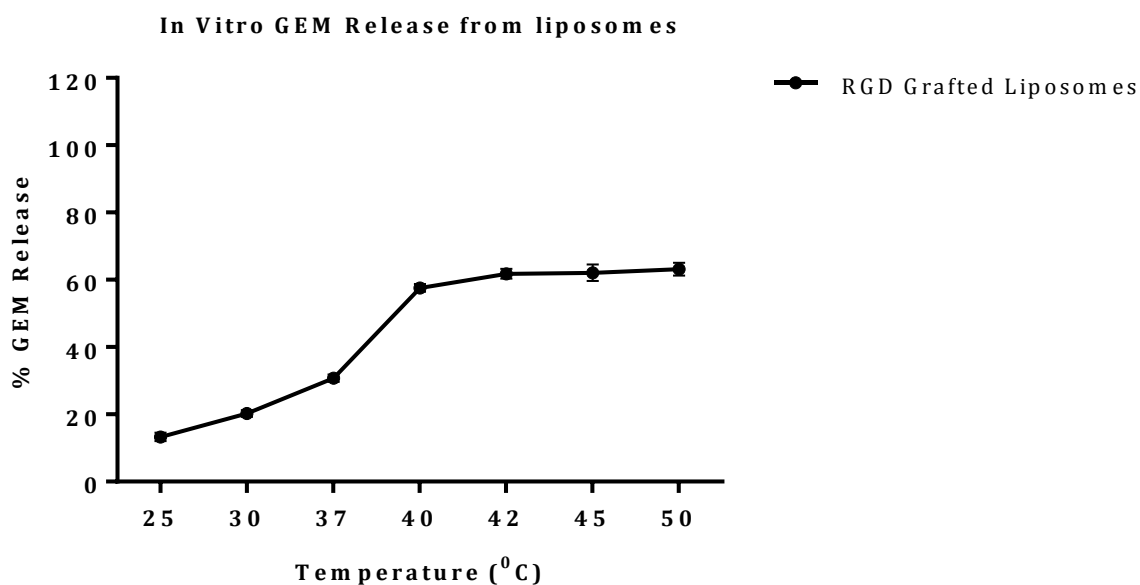
FIGURE 4 14. *In vitro* Release of GEM from Liposomes

The formulated GEM liposomsomes was chosen as the desired nanocarrier based on its ability to entrap high amount of GEM (entrapment efficiency of GEM is 62.05 ± 1.52 (%). Heat triggered release of liposomes was reported to be influenced by lipid composition and melting phase transition temperature (Tm) [16, 17]. At Tm, the structure of the lipid bilayer changes from a solid gel phase to a liquid-crystalline phase making the membrane more permeable to water and hydrophilic content of liposomes [18]. With DPPC as a major component (86% of lipids total weight, DPPC Tm is at 42°C), liposomes was found to be significantly stable at 37°C but very unstable around its Tm value. This observed behaviour of the liposomes clearly suggests how sensitive they are to temperatures between 39 -42°C with sharp release about 60% within 10 min at 42°C. This data is consistent with other GEM-loaded liposomes [15].

4.5. Haemolysis Study

Due to their resemblance with biological membranes liposomes are acceptable and essentially nontoxic to blood cells. But sometimes haemolytic activity is seen with the liposomal components [19-21]. It has been also reported that various lipids including short-chain phosphatidylcholines and lipid metabolites like free fatty acids and lysophosphatidylcholine induce erythrocyte lysis by some non-specific destruction of cell wall causing various Sodium(Na^+) and potassium(K^+) ion permeability defects [19, 22, 23]. This might be related to the haemolytic activity of various liposomes and lipid component due to lipid mediated pore formation. Such pore formation can induce haemoglobin leakage and consequent haemolysis.

Phospholipids are prone to undergo various physicochemical changes on exposure to different conditions[24, 25]. Chemically phospholipids are susceptible to hydrolytic reactions at the ester bonds. Hydrolysis induces formation of lysophosphatidylcholine and free fatty acids[26]and causes increase in membrane permeability[27]. Such changes also induce changes in organization of liposomes causing transformation to micellar solutions[27]. Such components as described earlier can cause erythrocyte lysis by getting incorporated in erythrocyte membrane and causing ion permeability defects. This necessitates the evaluation of haemolysis potential of liposomes.

Haemolytic toxicity of formulated liposomes was checked by incubating the formulation with Red Blood Cells separated from Rat blood by centrifugation at low speed [28] and analysing the samples for haemoglobin release at 541 nm [21]. The haemolysis with different formulations were compared with that obtained with Triton-X100 as a positive control[29].

Method

In vitro haemolysis test as described by Oku and Namba[21] was used with some modifications. Blood samples were collected in 2 mL Eppendorff tubes from the Sprague Dawley Rats by retroorbital puncture. All blood samples were heparinised. The blood samples were washed with normal saline (0.9 % w/w Sodium Chloride in water) 3 times before use to remove plasma components. For washing, each mL of blood samples was treated with 1 mL normal saline and gently stirred up and then centrifuged on Remi Lab Centrifuge at low speed (3000 rpm) to separate the red blood cells (RBCs). The RBC pellet separated was re-suspended in normal saline and washed the same way.

Final pellet was used to prepare 0.5 % v/v dispersion of RBCs based on the final volume. 25 µL of RBC pellet was re-suspended in 2 mL of normal saline taken in a 10 mL Centrifuge tube. Specific volumes of different liposomal formulations were sampled in these centrifuge tubes and the volume was made up to 5 mL with normal saline. This will make the final

concentration of RBCs 0.5 % v/v. Volumes of different liposome components/formulations were chosen to get the final concentrations to range from 0.01 µM to 10µM of lipid.

Positive Control was prepared by getting 100 % haemolysis of RBCs by using 0.5 % TritonX100 (20 µL in 5 mL) instead of formulation treatment. Negative Control was prepared by using the dilutions without any formulation treatment (Dilution only with normal saline).

Different components of liposomes were evaluated separately and incorporated in liposomes for their potential to cause haemolysis.

- Blank CLs
- CLs
- PLs
- RGD-grafted liposomes

Depending on the total lipid content of the each liposomal dispersion, appropriate volumes of each was used to treat blood cells to get semi-log concentration range. After treatment with each liposomal formulation, RBC dispersion was gently stirred for effective suspension of RBCs. The treated dispersions were incubated at 37°C for 30 min in incubator. After incubation all the samples were centrifuged at low speed (3000 rpm for 5 min) to separate the RBC mass and the solutions were analysed for UV absorbance at 541 nm wavelength against normal saline as a measure of haemolysis. Percentage of haemolysis was determined for different samples considering the absorbance value of sample treated with Triton-X100 to represent 100 % haemolysis.

4.5.1. Results and Discussion

The haemolysis observed with different formulations as compared to that with Triton-X100 are shown in **Table 4.12**. Relative haemolytic potentials are also shown graphically in **Figure 4.16**

TABLE 4 11. Haemolysis by Liposomes

| µM of lipid	%Relative Haemolysis					
	CLs		PLs		RGD-DDHC grafted Liposomes (3%)	
	Mean	SEM	Mean	SEM	Mean	SEM
0.01	2.645	0.450	2.140	0.199	1.850	0.110
0.1	6.200	0.400	4.251	0.501	3.875	0.750
1	10.250	0.350	4.358	0.485	4.105	0.850
10	14.950	0.550	4.782	0.750	4.687	0.650

Haemolysis of Liposomes
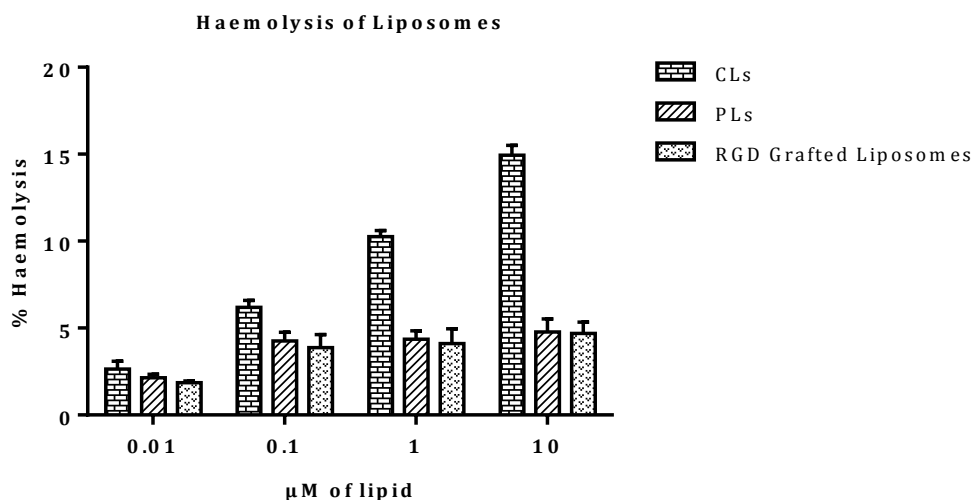
FIGURE 4 15. Haemolytic Potential of Liposomes

Hemolysis study was performed to investigate the potential toxicity after the intravenous injection of PLs, CL and RGD grafted liposomes in vivo. The leakage of hemoglobin was used to quantitatively compare the membrane-damaging properties of these liposomes. As shown in **Figure 4.16**, the conventional liposomes without PEG showed much higher extents of hemolysis rate than the PEGylated liposomes at all the concentration ($p < 0.05$). Without PEG, CL induced mild hemolysis ($\sim$15%). On the contrary, the hemolysis rates in all PEGylated liposomes were less than 5%. It is known that, PEG is a highly hydrated polymer and has a high degree of segmental flexibility in aqueous solution. Thus, PEGylation is commonly considered to reduce the serious cellular interaction [30, 31] and consequently reduce the damage to red blood cell. With the improved the biocompatibility, the PEGylated liposomes could be further explored for anti-tumor activity, cellular uptake and in vivo effect. Further RGD grafting has also shown minor reduction in haemolysis. At all concentrations haemolysis was found to be very less. Thus we conclude from the observations that optimized batches of PEGylated liposomes have very less potential to cause haemolysis at therapeutic concentrations of lipids body would be exposed.

4.6. Electrolyte induced flocculation test

Particle aggregation refers to formation of clusters in a colloidal suspension and represents the most frequent mechanism leading to destabilization of colloidal systems. During this process, which normally occurs within short periods of time (seconds to hours), particles dispersed in the liquid phase stick to each other, and spontaneously form irregular particle clusters, flocks, or aggregates. This phenomenon is also referred to as coagulation or flocculation and such dispersion is also called unstable. Particle aggregation can be induced by adding salts or another chemical referred to as coagulant or flocculant [32]. Some people

refer to specifically to flocculation when aggregation is induced by addition of polymers or polyelectrolytes, while coagulation is a more widely used term. Numerous experimental techniques have been developed to study particle aggregation. Most frequently used are time-resolved optical techniques that are based on transmittance or scattering of light[33]. Light scattering techniques are based on probing the scattered light from an aggregating suspension in a time-resolved fashion. Static light scattering yields the change in the scattering intensity, while dynamic light scattering the variation in the apparent hydrodynamic radius. At early-stages of aggregation, the variation of each of these quantities is directly proportional to the aggregation rate constant k[34]. At later stages, one can obtain information on the clusters formed (e.g., fractal dimension)[35]. Light scattering works well for a wide range of particle sizes. Multiple scattering effects may have to be considered, since scattering becomes increasingly important for larger particles or larger aggregates. Such effects can be neglected in weakly turbid suspensions. Aggregation processes in strongly scattering systems have been studied with backscattering techniques or diffusing-wave spectroscopy.

4.6.1. Method

Prepared liposomal formulations in three different categories, i.e. without pegylation, with pegylation and with RGD grafting, were studied for electrolyte induced flocculation test. This test confirms the stability of liposomal formulations in presence of electrolyte *in vivo*. This also proves the efficacy of pegylation effect governed by $mPEG_{2000}$-DSPE on the liposomal surface.1mL of liposomal suspensions were mixed with 4mL sodium chloride solution of different concentrations (1% to 5% w/v). The mixtures were then incubated in a shaker incubator at 37 °C with constant mild shaking for 2 hours to assess their electrolyte induced flocculation. Results are summarised in **Table 4.13.**

4.6.2. Results and Discussion

In the present study, the existence of a hydrated mPEG barrier on liposome surface was investigated by electrolyte flocculation study. This is based on the fact that the physical stability of a colloidal system is mainly dependent upon the competitive processes of attraction (vander Waals forces) and repulsion (either electrostatic repulsive force or steric stabilizing barrier or both). If particles are mainly stabilized electrostatically, destruction of the electrostatic double layer surrounding the particles will result in aggregation of the particles into clusters with a corresponding increase in optical turbidity. However, if the particles are mainly stabilized by a hydrated steric stabilizing barrier, the colloidal system should be stable even if the electrostatic double layers have been destroyed.

Sodium chloride is one of the most electrolytes used to check efficacy of pegylation. **Figure 4.17** depict changes in particle size at different concentration of sodium chloride. Salt induced flocculation measures the efficacy of steric hindrance provided by $mPEG_{2000}$-DSPE. Particle size of un-PEGylated liposomes was found to increase significantly at all concentration of added salt in liposomal formulations. Up to 3% NaCl addition was found to maintain particle size of PLs and RGD-grafted liposomes below 200 nm. Addition of three per cent and above concentration of salt increased the particle size up to 300 nm.

TABLE 4 12. Influence of sodium chloride concentration on mean particle size of liposomes

% NaCl	Particle Size (nm)					
	CLs		PLs liposomes		RGD-grafted Liposomes (3%)	
	Mean	SEM	Mean	SEM	Mean	SEM
0	148.221	2.155	146.225	2.011	142.118	2.170
1	180.145	2.149	142.114	2.150	146.214	2.014
2	210.214	3.515	147.158	1.449	145.147	1.147
3	302.211	2.415	175.157	2.199	182.236	2.221
4	375.145	4.258	255.128	1.950	278.258	2.412
5	450.541	2.501	308.147	4.149	318.147	3.850

Values are Mean±SD, n=3. CLs: Conventional liposomes; PLs: PEGylated liposomes. The mean particle size of CLs significantly increased ($p<0.05$) as compared to all PEGylated liposomes.
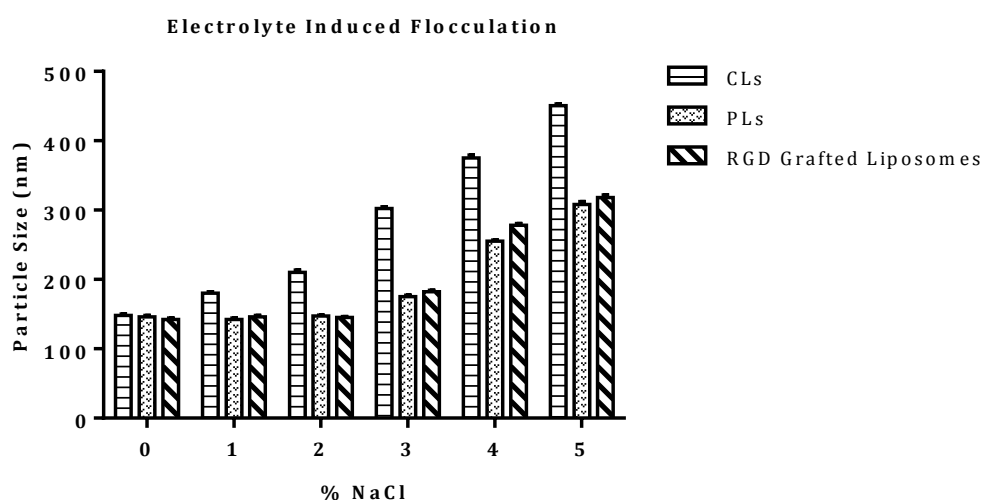

FIGURE 4 16. Electrolyte Induced Flocculation of Liposomes

Thus, prepared liposomal formulations of gemcitabine were found to be stable in presence of electrolytes.

4.7 References

1. Berridge, M.V., P.M. Herst, and A.S. Tan, *Tetrazolium dyes as tools in cell biology: new insights into their cellular reduction.* Biotechnol Annu Rev, 2005. **11**: p. 127-52.

2. Berridge, M.V. and A.S. Tan, *Characterization of the cellular reduction of 3-(4,5-dimethylthiazol-2-yl)-2,5-diphenyltetrazolium bromide (MTT): subcellular localization, substrate dependence, and involvement of mitochondrial electron transport in MTT reduction.* Arch Biochem Biophys, 1993. **303**(2): p. 474-82.

3. Van Dilla, M.A., et al., *Cell microfluorometry: a method for rapid fluorescence measurement.* Science, 1969. **163**(3872): p. 1213-4.

4. Lauer, S.A. and J.P. Nolan, *Development and characterization of Ni-NTA-bearing microspheres.* Cytometry, 2002. **48**(3): p. 136-45.

5. Baserga, R., *13 - Recombinant DNA Approaches to Studying Control of Cell Proliferation: An Overview*, in *Recombinant Dna and Cell Proliferation*, G.S.S.L. Stein, Editor. 1984, Academic Press. p. 337-350.

6. Hochhauser, S.J., J.L. Stein, and G.S. Stein, *Gene expression and cell cycle regulation.* Int Rev Cytol, 1981. **71**: p. 95-243.

7. Baserga, R., *Growth in size and cell DNA replication.* Exp Cell Res, 1984. **151**(1): p. 1-5.

8. Tyson, J.J., *The coordination of cell growth and division — intentional or Incidental?* BioEssays, 1985. **2**(2): p. 72-77.

9. Kerker, M., et al., *Is the central dogma of flow cytometry true: that fluorescence intensity is proportional to cellular dye content?* Cytometry, 1982. **3**(2): p. 71-8.

10. Danhier, F., A. Le Breton, and V. Preat, *RGD-based strategies to target alpha(v) beta(3) integrin in cancer therapy and diagnosis.* Mol Pharm, 2012. **9**(11): p. 2961-73.

11. Bepler, G., et al., *RRM1 modulated in vitro and in vivo efficacy of gemcitabine and platinum in non-small-cell lung cancer.* J Clin Oncol, 2006. **24**(29): p. 4731-7.

12. Lyseng-Williamson, K.A. and C. Fenton, *Docetaxel: a review of its use in metastatic breast cancer.* Drugs, 2005. **65**(17): p. 2513-31.

13. Saloustros, E., D. Mavroudis, and V. Georgoulias, *Paclitaxel and docetaxel in the treatment of breast cancer.* Expert Opin Pharmacother, 2008. **9**(15): p. 2603-16.

14. McGuire, W.P., 3rd and M. Markman, *Primary ovarian cancer chemotherapy: current standards of care.* Br J Cancer, 2003. **89 Suppl 3**: p. S3-8.

15. Lim, S.K., et al., *Enhanced antitumor efficacy of gemcitabine-loaded temperature-sensitive liposome by hyperthermia in tumor-bearing mice.* Drug Dev Ind Pharm, 2014. **40**(4): p. 470-6.

16. Hossann, M., et al., *In vitro stability and content release properties of phosphatidylglyceroglycerol containing thermosensitive liposomes.* Biochim Biophys Acta, 2007. **1768**(10): p. 2491-9.

17. Kneidl, B., et al., *Thermosensitive liposomal drug delivery systems: state of the art review.* Int J Nanomedicine, 2014. **9**: p. 4387-98.

18. Grull, H. and S. Langereis, *Hyperthermia-triggered drug delivery from temperature-sensitive liposomes using MRI-guided high intensity focused ultrasound.* J Control Release, 2012. **161**(2): p. 317-27.

19. Lundbaek, J.A. and O.S. Andersen, *Lysophospholipids modulate channel function by altering the mechanical properties of lipid bilayers.* J Gen Physiol, 1994. **104**(4): p. 645-73.

20. Niki, E., et al., *Oxidative hemolysis of erythrocytes and its inhibition by free radical scavengers.* J Biol Chem, 1988. **263**(36): p. 19809-14.

21. Oku, N. and Y. Namba, *Glucuronate-modified, long-circulating liposomes for the delivery of anticancer agents.* Methods Enzymol, 2005. **391**: p. 145-62.

22. Bierbaum, T.J., S.R. Bouma, and W.H. Huestis, *A mechanism of erythrocyte lysis by lysophosphatidylcholine.* Biochim Biophys Acta, 1979. **555**(1): p. 102-10.

23. Tanaka, Y., et al., *Mechanism of human erythrocyte hemolysis induced by short-chain phosphatidylcholines and lysophosphatidylcholine.* J Biochem, 1983. **94**(3): p. 833-40.

24. Grit, M. and D.J. Crommelin, *Chemical stability of liposomes: implications for their physical stability.* Chem Phys Lipids, 1993. **64**(1-3): p. 3-18.

25. Heurtault, B., et al., *Physico-chemical stability of colloidal lipid particles.* Biomaterials, 2003. **24**(23): p. 4283-300.

26. Zuidam, N.J. and D.J.A. Crommelin, *Differential scanning calorimetric analysis of dipalmitoylphosphatidylcholine-liposomes upon hydrolysis.* International Journal of Pharmaceutics, 1995. **126**(1–2): p. 209-217.

27. Zuidam, N.J., et al., *Physical (in) stability of liposomes upon chemical hydrolysis: the role of lysophospholipids and fatty acids.* Biochim Biophys Acta, 1995. **1240**(1): p. 101-10.

28. Bosch, F.H., et al., *Characteristics of red blood cell populations fractionated with a combination of counterflow centrifugation and Percoll separation.* Blood, 1992. **79**(1): p. 254-60.

29. Prete, P.S., et al., *Quantitative assessment of human erythrocyte membrane solubilization by Triton X-100.* Biophys Chem, 2002. **97**(1): p. 1-5.

30. Ding, H., et al., *Bioconjugated PLGA-4-arm-PEG branched polymeric nanoparticles as novel tumor targeting carriers.* Nanotechnology, 2011. **22**(16): p. 165101.

31. Wang, W., et al., *Protective effect of PEGylation against poly(amidoamine) dendrimer-induced hemolysis of human red blood cells.* J Biomed Mater Res B Appl Biomater, 2010. **93**(1): p. 59-64.

32. Elimelech, M., *Particle deposition and aggregation : measurement, modelling, and simulation.* Colloid and surface engineering series. 1995, Oxford England ; Boston: Butterworth-Heinemann. xv, 441 p.

33. Gregory, J., *Monitoring particle aggregation processes.* Adv Colloid Interface Sci, 2009. **147-148**: p. 109-23.

34. Holthoff, H., et al., *Measurement of Absolute Coagulation Rate Constants for Colloidal Particles: Comparison of Single and Multiparticle Light Scattering Techniques.* J Colloid Interface Sci, 1997. **192**(2): p. 463-70.

35. Lin, M.Y., et al., *Universality in colloid aggregation.* Nature, 1989. **339**(6223): p. 360-362.